Minimizing State-of-Health Degradation in Hybrid Electrical Energy Storage Systems with Arbitrary Source and Load Profiles

***Abstract*—Hybrid electrical energy storage (HEES) systems consisting of heterogeneous electrical energy storage (EES) elements are proposed to exploit the strengths of different EES elements and hide their weaknesses for achieving a combination of superior performance metrics. The cycle life of the EES elements is one of the most important metrics that should be considered carefully. The cycle life is directly related to the state-of-health (SoH), which is defined as the ratio of full charge capacity of an aged EES element to its designed (or nominal) capacity. The SoH degradation models of battery in the previous literature can only be applied to charging/discharging cycles with the same state-of-charge (SoC) swing. To address this shortcoming, this paper derives a novel SoH degradation model of battery for charging/discharging cycles with arbitrary patterns. Based on the proposed model, this paper presents a near-optimal charge management policy focusing on extending the cycle life of battery elements in the HEES systems while simultaneously improving the overall cycle efficiency. The SoH-aware charge management policy is based on convex optimization technique. Experimental results show significant cycle life enhancement up to 17.3X.**

I. INTRODUCTION

Electrical energy storage (EES) systems are deployed to increase power availability, reliability and efficiency, mitigate the supply-demand mismatch, and regulate the peak-power demand [1][2]. Unfortunately, none of the existing EES elements, such as Li-ion batteries, lead-acid batteries, and supercapacitors, can simultaneously fulfill all the desirable performance metrics, e.g., long cycle life, high power and energy densities, low cost/weight per unit capacity, high cycle efficiency, and low environmental effects. This discourages the wide spread of large-scale EES systems.

Hybrid EES (HEES) systems consisting of heterogeneous EES elements are proposed to exploit the strengths of different EES elements and hide their weaknesses for achieving a combination of superior performance metrics [3][4]. For a HEES system to be useful in practice, it is essential to efficiently implement three management operations: charge allocation, charge replacement, and charge migration [5][6][7].

Among all the performance metrics, the cycle life of the EES elements is one of the most important metrics that should be considered carefully. The cycle life is directly related to the state-of-health (SoH), which is defined as the ratio of full charge capacity of an aged EES element to its designed (or nominal) capacity. This metric captures the "health" condition of the EES elements, i.e., their ability to store and deliver energy compared to a fresh new one.

The SoH degradation models of battery in the previous literature can only be applied to charging/discharging cycles with same state-of-charge (SoC) swing[1] [8][9]. To address this shortcoming, we derive a novel SoH degradation model of battery for charging/discharging cycles with arbitrary patterns. The proposed SoH degradation model is based on an important observation: both a higher SoC swing and a higher average SoC in the charging/discharging cycles will result in a higher SoH degradation rate.

Some references have worked on extending the cycle life of EES elements [10][11][12]. However, they only focus on either a single EES element or a homogeneous EES system, which consists of only one type of EES element. Different from a single EES element or a homogeneous EES system, the cycle life of the EES elements in a HEES system is largely dependent on the HEES charge management policy. A recent work [13] proposes an SoH-aware charge management policy for the HEES systems based on the SoH degradation model introduced in [8]. It uses the supercapacitor bank as a buffer to shave the spiky portion of the source or load profiles so that the battery bank can stably receive energy from power source or provide energy to load device. This charge management policy has the following limitations: (i) it can only be applied to a two-bank HEES architecture consisting of a battery bank and a supercapacitor bank, (ii) it is only effective for source or load profiles in periodic patterns due to the limitation of the SoH degradation model from [8], and (iii) it is based on a simple crossover filter and is far from optimal.

In this work, based on our novel SoH degradation model, we derive a near-optimal charge management policy focusing on extending the cycle life of battery elements in the HEES systems while simultaneously improving the overall cycle efficiency. The SoH-aware charge management policy is based on convex optimization techniques, and has the following extensions over [13]:

- It is applicable to the general HEES architecture consisting of multiple battery banks and multiple supercapacitor banks.
- It can be applied for source and load profiles with arbitrary patterns and is no longer limited to profiles in periodic patterns.
- It achieves higher performance, because the optimization of charging/discharging currents of various EES banks depends not only on the frequency components but also on the magnitudes of the source and load profiles. However, the policy in [13] only depends on the frequency components.

II. HEES SYSTEM ARCHITECTURE AND MANAGEMENT

The general HEES system architecture is proposed in [5]. The system comprises multiple different EES banks, connected with each other through the *Charge Transfer Interconnect* (CTI). Each EES bank consists of an EES (element) array and a *bidirectional converter*. The EES array is composed of multiple homogeneous EES elements with the same SoC, organized in a two-dimensional array using series and/or parallel connections. The bidirectional converter controls power transfer into and out of the EES array through the CTI. The bidirectional converter is typically implemented based on a switching-mode power converter and can be configured in either voltage or current regulating mode.

An HEES system uses a main controller to determine the operation of converters [5]. The main controller determines the voltage level of the CTI, the charging/discharging current of each EES bank, and the current drawn from the power source according to charge management policies. We set only one converter in the voltage regulating mode and let it control the CTI voltage. All the others operate in the current regulating mode. The output current of the voltage regulating converter is automatically determined so that the sum of currents flowing into the CTI is equal to the sum of currents flowing out. Feedback control loops are employed in the converters to maintain the stability of their output voltage/current, and the main controller provides high-level charge management policies.

III. SOH DEGRADATION MODEL

First, we formally define the SoC and SoH degradation of an EES array. The SoC of an EES array is defined by

$$SoC = \frac{C_{array}}{C_{full}} \times 100\% \quad (1)$$

where C_{array} is the amount of charge stored in the EES array, and C_{full} is the amount of charge in the EES array when it is fully charged. We interpret SoC as the state of the EES array. On the other hand, the C_{full} value gradually decreases during battery aging (i.e., SoH degradation.) The amount of SoH degradation, denoted by D_{SoH}, is defined as follows:

[1] SoC is defined as the available capacity remaining in the EES element, expressed as a percentage of the rated capacity. SoC swing is defined as the SoC fluctuation during a charging/discharging cycle.

$$D_{SoH} = \frac{C_{full}^{nom} - C_{full}}{C_{full}^{nom}} \times 100\% \quad (2)$$

where C_{full}^{nom} is nominal value of C_{full} for a fresh new EES array.

A. Related Work

The battery capacity fading (i.e., SoH degradation) results from long-term electrochemical reaction, which involves the carrier concentration loss and internal impedance growth in batteries. These effects strongly depend on the operating condition of the battery such as charging/discharging current, number of cycles, SoC swing, average SoC, and operation temperature [9][14]. The characterization of battery capacity fading requires exhausting and time-consuming experiments. Therefore, the accurate electrochemistry-based models [15][16] have been developed for battery capacity fading. However, they are difficult to use in practice due to the complexity. On the other hand, mathematical models provide us an effective and efficient way to estimating the SoH degradation. Hence, we discuss in the following the SoH degradation model of Li-ion batteries proposed in [8], which shows a good match with real data but can only be applied to charging and discharging cycles with the same SoC swing. After that we propose a novel SoH degradation model that can be applied to charging and discharging cycles with arbitrary patterns.

The SoH degradation model in [8] estimates the SoH degradation of a Li-ion battery for cycled charging/discharging, where a (charging/discharging) *cycle* is defined as a charging process of the battery cell from SoC_{low} to SoC_{high} and a discharging process following it from SoC_{high} to SoC_{low}. The SoH degradation during one cycle depends on the *average SoC level* SoC_{avg} and the *SoC swing* SoC_{swing}. We calculate SoC_{avg} and SoC_{swing} in one cycle as:

$$SoC_{avg} = (SoC_{low} + SoC_{high})/2 \quad (3)$$

$$SoC_{swing} = SoC_{high} - SoC_{low} \quad (4)$$

SoC_{swing} reaches the maximum value of 1.0 (100%) in a full (100% depth) cycle, i.e., the SoC changes from 0 to 100% and then back to 0.

The SoH degradation $D_{SoH,cycle}$ during one charging/discharging cycle, depending on both SoC_{avg} and SoC_{swing}, is given by

$$\begin{aligned} D_1 &= K_{co} \cdot \exp\left[(SoC_{swing} - 1) \cdot \frac{T_{ref}}{K_{ex} \cdot T_B}\right] + 0.2\frac{\tau}{\tau_{life}} \\ D_2 &= D_1 \cdot \exp\left[4K_{SoC} \cdot (SoC_{avg} - 0.5)\right] \cdot (1 - D_{SoH}) \\ D_{SoH,cycle} &= D_2 \cdot \exp\left[K_T \cdot (T_B - T_{ref}) \cdot \frac{T_{ref}}{T_B}\right] \end{aligned} \quad (5)$$

where K_{co}, K_{ex}, K_{SoC}, and K_T are battery specific parameters; T_B and T_{ref} are the battery temperature and reference battery temperature, respectively; τ is the duration of this charging/discharging cycle; τ_{life} is the calendar life of the battery. We use $D_{SoH,cycle}(SoC_{swing}, SoC_{avg})$ to denote $D_{SoH,cycle}$ as a function of SoC_{swing} and SoC_{avg}. The total SoH degradation (from a new battery) after M charging/discharging cycles is calculated by

$$D_{SoH} = \sum_{m=1}^{M} D_{SoH,cycle}(m) \quad (6)$$

where $D_{SoH,cycle}(m)$ denotes the SoH degradation in the m^{th} cycle.

In (6), D_{SoH} increases from 0 (brand new) to 100% (no capacity left). Typically, the value of $D_{SoH} = 20\%$, which indicates 80% remaining capacity left in the battery, are used in the literature to represent end of life. Figure 1 reflects the cycle life of a Li-ion battery under different SoC_{swing} and SoC_{avg}. In this experiment, we vary the SoC fluctuation range (i.e., SoC_{low} and SoC_{high}) in a cycle to achieve different SoC_{swing} and SoC_{avg} (from (3) and (4)). The charging and discharging cycles are repeated until the battery reaches $D_{SoH} = 20\%$, and then we record the total number of cycles finished (i.e., the *cycle life* of the battery). There are two important observations from Figure 1: (i) both higher SoC swing and higher average SoC in the charging/discharging cycles can result in a higher SoH degradation rate, (ii) the cycle life of a Li-ion battery increases superlinearly with respect to the reduction of SoC swing and average SoC. We make use of these observations as well as the function $D_{SoH,cycle}(SoC_{swing}, SoC_{avg})$ in the proposed SoH degradation model and SoH-aware charge management algorithm.

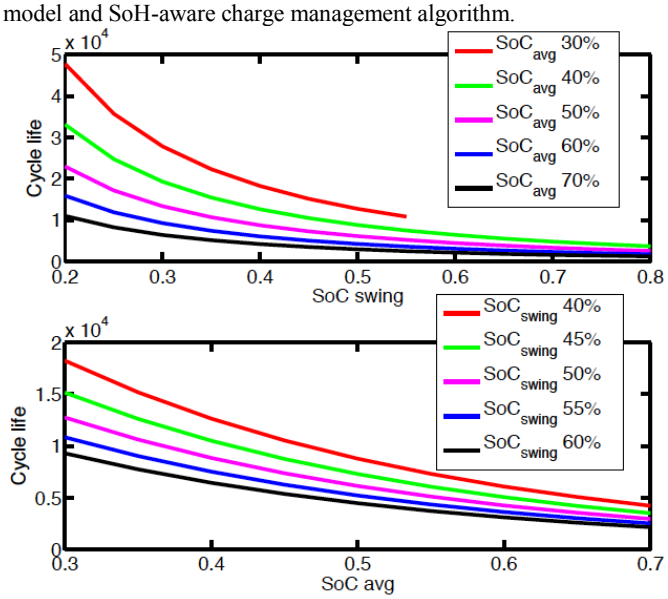

Figure 1: Li-ion battery cycle life versus SoC swing (at different average SoC levels) and average SoC level (at different SoC swings).

The SoH degradation of lead-acid batteries satisfies a similar relationship with respect to the average SoC and the SoC swing [17]. However, the SoH degradation rate of lead-acid batteries is much higher than that of Li-ion batteries. A typically lead-acid battery has a cycle life of 300 – 500 cycles when $SoC_{swing} = 100\%$, whereas the cycle life of a Li-ion battery is around 1500 – 2500 cycles [3]. On the other hand, the supercapacitors have a cycle life that is orders of magnitude higher than batteries [3]. Hence, we do not consider the SoH degradation of supercapacitors in this paper.

B. Proposed SoH Degradation Model

In this section, we derive a novel SoH degradation model, which can be applied to charging/discharging cycles with arbitrary patterns. The proposed novel SoH degradation model extends and generalizes the SoH degradation model introduced in [8] based on the following two observations:

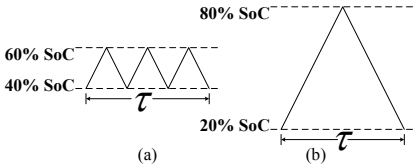

Figure 2: Illustrative example of Observation I.

Observation I: The SoH degradation rate is a superlinear function of the SoC swing SoC_{swing} and the average SoC level SoC_{avg} as can be seen from the discussion in Section III.A. Moreover, the SoC swing has dominant effect over the average SoC level.

An illustrative example of Observation I is provided in Figure 2, which shows two SoC profiles of a battery within the same time duration of τ. In Figure 2(a) there is three cycles each with a SoC swing of 20% and an average SoC of 50%, while in Figure 2(b) there is one cycle with a SoC swing of 60% and an average SoC of 50%. The SoC profile in Figure 2(b) results in a much higher SoH degradation (about 71.6% higher) though it has a smaller number of charging/discharging cycles.

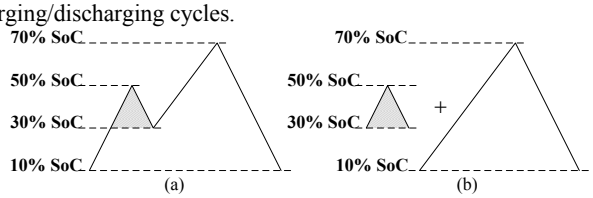

Figure 3: Illustrative example of Observation II.

Observation II (Decoupling of Cycles): Consider the SoC profile of a battery cell in Figure 3(a). Although it is not possible to directly apply the model in [8] to estimate the SoH degradation, we can perceive it as a combination of two charging/discharging cycles as shown in Figure 3(b). Figure 3(a) and 3(b) are equivalent in terms of the SoC swing and the average SoC, which are the two critical factors determining the SoH degradation.

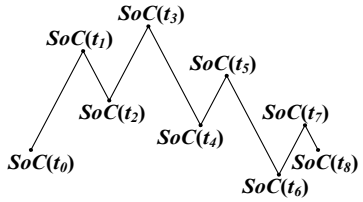

Figure 4: An example battery SoC profile versus time and the set of turning points.

Based on the two observations, we provide the general SoH degradation model as follows. Consider a period $[0, \tau]$ of charge management. We assume that the duration of the period is too small compared with the battery lifetime (300 – 500 cycles for lead-acid battery or 1500 – 2500 cycles for Li-ion battery [3]) to make any noticeable change in the C_{full}. Let $D_{SoH,period}$ denote the total SoH degradation of the Li-ion battery over this period, which we are going to estimate. In the first step, we initialize the value of $D_{SoH,period}$ to zero. We identify a set of *turning points* t_1, t_2, ..., t_n, at which points the battery changes from charging to discharging or from discharging to charging. Figure 4 shows an example SoC profile versus time of a battery element and the set of turning points.

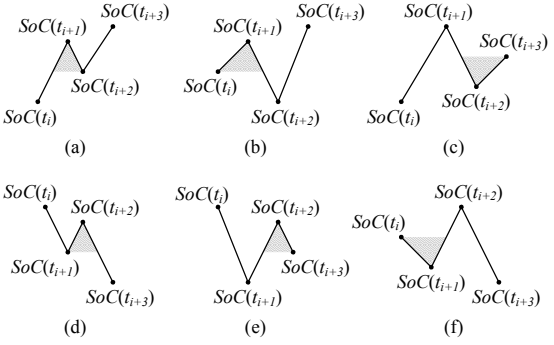

Figure 5: Six basic cases for (charging/discharging) cycle identifcation.

Next, we identify four consecutive turning points $(t_i, t_{i+1}, t_{i+2}, t_{i+3})$ from the set of turning points, satisfying one of the following six cases:

(a) $SoC(t_i) \le SoC(t_{i+2}) < SoC(t_{i+1}) \le SoC(t_{i+3})$,

(b) $SoC(t_{i+2}) < SoC(t_i) < SoC(t_{i+1}) \le SoC(t_{i+3})$,

(c) $SoC(t_i) \le SoC(t_{i+2}) < SoC(t_{i+3}) < SoC(t_{i+1})$,

(d) $SoC(t_{i+3}) \le SoC(t_{i+1}) < SoC(t_{i+2}) \le SoC(t_i)$,

(e) $SoC(t_{i+1}) < SoC(t_{i+3}) < SoC(t_{i+2}) \le SoC(t_i)$,

(f) $SoC(t_{i+3}) \le SoC(t_{i+1}) < SoC(t_i) < SoC(t_{i+2})$,

The six cases are shown in Figure 5(a) - (f). In each case, we identify a complete charging/discharging cycle as shown by the shadowed area in Figure 5(a) - (f). We take case (a) as an example. The SoC swing and average SoC level of the identified charging/discharging cycle (labeled by the shade) are given by:

$$SoC_{swing} = SoC(t_{i+1}) - SoC(t_{i+2}) \tag{7}$$

$$SoC_{avg} = \frac{SoC(t_{i+1}) + SoC(t_{i+2})}{2} \tag{8}$$

Then we estimate the SoH degradation in this cycle by $D_{SoH,cycle}(SoC_{swing}, SoC_{avg})$. We delete the cycle labeled by the shade and update the value of $D_{SoH,period}$ using:

$$D_{SoH,period} \leftarrow D_{SoH,period} + D_{SoH,cycle}(SoC_{swing}, SoC_{avg}) \tag{9}$$

The updating procedures of $D_{SoH,period}$ in the other five cases are similar and thus not explained in detail. We continue this procedure until only one cycle, i.e., the cycle with the largest SoC swing, remains in the SoC profile of the battery. Then we obtain an effective estimate value of $D_{SoH,period}$. Figure 6 provides an example of estimating the $D_{SoH,period}$ value from a battery SoC profile.

It is provable that charging/discharging cycles with arbitrary patterns can be decoupled using this procedure to a set of charging/discharging cycles with potentially different SoC swings and different average SoC levels. Therefore, we effectively calculate $D_{SoH,period}$ using this decoupling procedure. The details of proof are omitted due to space limitation. Please note that although this SoH degradation model cannot be as accurate as an electrochemical model, it provides enough insight for guiding the SoH-aware charge management in HEES systems since it is based on the two important observations about the SoH degradation.

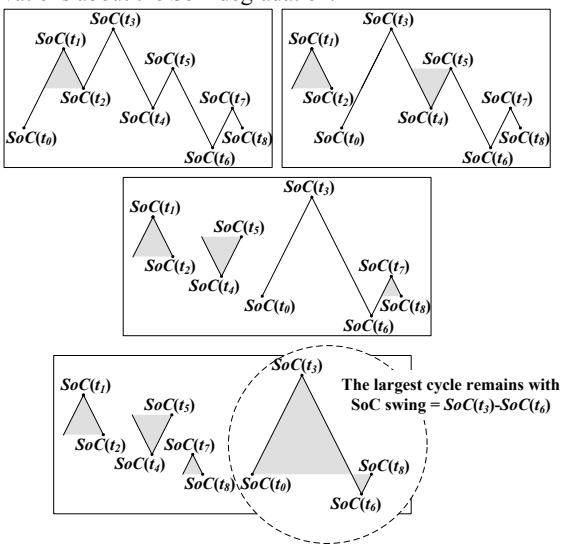

Figure 6: An example of estimating the $D_{SoH,period}$ value from an arbitrary battery SoC profile.

IV. SoH-Aware Charge Management I: System Model and Problem Formulation

A. System Architecture

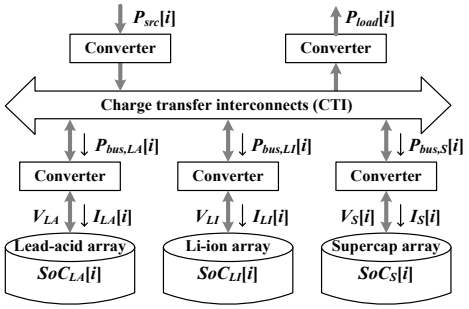

Figure 7: Structure of the HEES system considered in this paper.

Figure 7 presents the HEES system architecture, which consists of a lead-acid battery bank, a Li-ion battery bank, and a supercapacitor bank. The proposed charge management algorithm can handle more complicated HEES systems. Generally, lead-acid batteries are much cheaper than Li-ion batteries, yet they suffer from a shorter cycle life and incur higher power loss during charging and discharging due to more severe rate capacity effect. Supercapacitors are more expensive than both types of batteries. However, supercapacitors have nearly 100% charging and discharging efficiencies and an orders-of-magnitude longer cycle life than batteries.

We use a *slotted time model*, i.e., all the system constraints as well as decisions are provided for discrete time intervals of equal length. More specifically, the whole time period of charge management is divided into N time slots, each of duration Δ_T. The HEES charge

management algorithm should correctly account for the distinct characteristics of different types of EES elements and power dissipation in the DC-DC conversion circuitries.

B. System Power Model

Let $P_{src}[i]$ and $P_{load}[i]$ $(1 \le i \le N)$ denote power generation of the power source and power consumption of the electric load, respectively. Let $SoC_{LA}[i]$, $SoC_{LI}[i]$, and $SoC_S[i]$ denote the SoC values of the lead-acid battery array, the Li-ion battery array, and the supercapacitor array, respectively. Let V_{LA} and V_{LI} denote the terminal voltages of the lead-acid battery array and the Li-ion battery array, respectively. We neglect the dependency of the battery terminal voltages on the SoC values because the terminal voltages are nearly constant in the major SoC operation range of 20% to 80% [18]. On the other hand, let $V_S[i]$ denote the terminal voltage of the supercapacitor element array at time slot i, which is a linear function of SoC. Moreover, the charging/discharging currents of the lead-acid battery array, the Li-ion battery array, and the supercapacitor array are denoted by $I_{LA}[i]$, $I_{LI}[i]$, and $I_S[i]$, respectively. The current values are positive when charging the EES array and negative when discharging.

The *rate capacity effect* of batteries explains that the charging and discharging efficiencies decrease with the increasing of charging and discharging currents, respectively. More precisely, the Peukert's formula [18] describes that the charging and discharging efficiencies of a battery element array, as functions of the charging current I_c and discharging current I_d, respectively, are given by

$$\eta_{rate,c}(I_c) = \frac{k_c}{(I_c)^{\alpha_c}}, \quad \eta_{rate,d}(I_d) = \frac{k_d}{(I_d)^{\alpha_d}} \tag{10}$$

where k_c, α_c, k_d, and α_d are constants known *a priori*. We define the equivalent current inside the battery array as the actual charge accumulating/reducing speed inside the battery array. We calculate the equivalent current $I_{eq,LA}$ for the lead-acid battery array by:

$$I_{eq,LA} = \begin{cases} I_{LA} \cdot \eta_{rate,c,LA}(I_{LA}), & \text{if } I_{LA} > 0, \\ I_{LA} / \eta_{rate,d,LA}(|I_{LA}|), & \text{if } I_{LA} < 0. \end{cases} \tag{11}$$

The equivalent current of the Li-ion battery array can be calculated in the similar way. Lead-acid batteries are subject to a much more severe rate capacity effect compared with Li-ion batteries. On the other hand, the supercapacitor arrays have negligible rate capacity effect, i.e., $I_{eq,S} \approx I_S$.

For the lead-acid battery array, we calculate $SoC_{LA}[i]$ from the initial SoC $SoC_{LA}[1]$ using *Coulomb counting*:

$$SoC_{LA}[i] = SoC_{LA}[1] + \frac{\sum_{j=1}^{i-1} I_{eq,LA}[j] \cdot \Delta_T}{C_{full,LA}} \tag{12}$$

where $C_{full,LA}$ is the full charge capacity of the lead-acid battery array. Similar notations also apply for the Li-ion battery and the supercapacitor by replacing the subscript LA by LI and S, respectively.

The power conversion circuitries exploited in the system consume a significant portion of power. We denote the power conversion efficiencies ($< 100\%$ due to power consumption) of various converters at the i^{th} time slot by $\eta_{conv,LA}$, $\eta_{conv,LI}$, $\eta_{conv,S}$, $\eta_{conv,src}$, and $\eta_{conv,load}$. We use $P_{bus,LA}[i]$, $P_{bus,LI}[i]$, and $P_{bus,S}[i]$ $(1 \le i \le N)$ to denote the power flowing into the lead-acid battery bank, the Li-ion battery bank, and the supercapacitor bank from the CTI, respectively. $P_{bus,LA}[i]$ satisfies the following equation:

$$P_{bus,LA}[i] = \begin{cases} V_{LA} \cdot I_{LA}[i] / \eta_{conv,LA}, & \text{if } I_{LA}[i] > 0, \\ V_{LA} \cdot I_{LA}[i] \cdot \eta_{conv,LA}, & \text{if } I_{LA}[i] < 0. \end{cases} \tag{13}$$

$P_{bus,LI}[i]$ and $P_{bus,S}[i]$ also satisfy similar relationships. Moreover, we have the following equation due to the energy conservation law:

$$P_{bus,LA}[i] + P_{bus,LI}[i] + P_{bus,S}[i] = P_{src}[i] \cdot \eta_{conv,src} - \frac{P_{load}[i]}{\eta_{conv,load}} \tag{14}$$

C. Problem Formulation

The objective of the SoH-aware HEES system control algorithm is to minimize the SoH degradation while satisfying the load power requirements. However, since there are two types of batteries in the HEES system, we define a new objective function, the *overall value degradation*, which captures the different cycle lives and capital cost values of the two types of batteries. We define the overall value degradation during the period of charge management as follows. Let $D_{SoH,period,LA}$ and $D_{SoH,period,LI}$ denote the SoH degradation of the lead-acid battery array and Li-ion battery array during the period of charge management, respectively. Let $D_{SoH,end}$ denote the amount of SoH degradation indicating the end-of-life of a battery array (i.e., $D_{SoH,end} = 20\%$). The capital cost values of the lead-acid battery array and the Li-ion battery array are given by $Cost_{LA}$ and $Cost_{LI}$, respectively. Then the overall value degradation is

$$Cost_{LA} \cdot \frac{D_{SoH,period,LA}}{D_{SoH,end}} + Cost_{LI} \cdot \frac{D_{SoH,period,LI}}{D_{SoH,end}} \tag{15}$$

The SoH-aware HEES system control problem is formally described as follows:

Given: Power source and load device power profiles $P_{src}[i]$, $P_{load}[i]$, respectively, for $1 \le i \le N$, initial SoC's of the supercapacitor array $SoC_S[1]$.

Optimization variables: Initial SoC's of the two battery arrays $SoC_{LA}[1]$ and $SoC_{LI}[1]$, EES array charging/discharging currents $I_{LA}[i]$, $I_{LI}[i]$, $I_S[i]$ for $1 \le i \le N$.

Minimize: the overall value degradation given by Eqn. (15).

Subject to:

i) *Load Power Requirement Constraint*: (14) is satisfied.

ii) *Capacity and Power Rating Constraints*: Each EES array SoC cannot be less than zero or more than 100%, i.e.,

$$0 \le SoC_{LA}[i], SoC_{LI}[i], SoC_S[i] \le 100\% \tag{16}$$

Moreover, the charging/discharging current of each EES array cannot exceed a maximum value, i.e.,

$$-I_{LA,MAX,d} \le I_{LA}[i] \le I_{LA,MAX,c} \tag{17}$$

$$-I_{LI,MAX,d} \le I_{LI}[i] \le I_{LI,MAX,c} \tag{18}$$

$$-I_{S,MAX,d} \le I_S[i] \le I_{S,MAX,c} \tag{19}$$

iii) *Final Stored Energy Constraints*: Each EES array SoC at the end of the charge management period should be no less than the initial SoC value, i.e.,

$$SoC_{LA}[N+1] \ge SoC_{LA}[1], SoC_{LI}[N+1] \ge SoC_{LI}[1], SoC_S[N+1] \ge SoC_S[1] \tag{20}$$

V. SoH-Aware Charge Management II: Algorithm

We derive a near-optimal SoH-aware charge management policy based on the convex optimization technique. We need to find the near-optimal values of the initial SoC's $SoC_{LA}[1]$ and $SoC_{LI}[1]$, as well as the EES array current profiles $I_{LA}[i]$, $I_{LI}[i]$, $I_S[i]$ for $1 \le i \le N$. The proposed optimization method consists of an outer loop and a kernel algorithm. The outer loop finds near-optimal values of $SoC_{LA}[1]$ and $SoC_{LI}[1]$ using the ternary search technique, in order to minimize the overall value degradation while satisfying load power requirement (14). The kernel algorithm finds the optimal EES array current profiles $I_{LA}[i]$, $I_{LI}[i]$, $I_S[i]$ for $1 \le i \le N$. The general procedure to derive the SoH-aware charge management policy is shown in Algorithm 1. In the rest of this section, we describe the kernel algorithm in detail.

Algorithm 1: Deriving the SoH-aware charge management policy.

Perform ternary search to find the optimal $SoC_{LA}[1]$ and $SoC_{LI}[1]$:

> *The kernel algorithm:*
> Step I: Feasibility check.
> Step II: Derive the optimal EES array current profiles $I_{LA}[i]$, $I_{LI}[i]$, $I_S[i]$ for $1 \le i \le N$ to minimize the overall value degradation, given by Eqn. (15).

Find the optimal values of all optimization variables, such that the overall value degradation is minimized and constraints are satisfied.

A. The Kernel Algorithm

The kernel algorithm consists of two steps: Feasibility check and the subsequent optimization of EES array current profiles. We discuss these two steps as follows.

1) Feasibility Check

In this step, we are given the $SoC_{LA}[1]$ and $SoC_{LI}[1]$ values from the outer loop. We perform feasibility check, i.e. check whether it is possible to find the EES array current profiles $I_{LA}[i]$, $I_{LI}[i]$, $I_S[i]$ for $1 \le i \le N$ such that all the constraints (14), (16) – (20) are satisfied. We formulate the feasibility check problem as a convex constraint satisfaction problem (convex CSP) and optimally solve this problem in polynomial time.

First, we define the *energy increasing/decreasing rates* inside the lead-acid battery array, the Li-ion battery array, and the supercapacitor array by $P_{eq,LA}[i]$, $P_{eq,LI}[i]$, and $P_{eq,S}[i]$, respectively, satisfying:

$$P_{eq,LA}[i] = V_{LA} \cdot I_{eq,LA}[i] \tag{21}$$

$$P_{eq,LI}[i] = V_{LI} \cdot I_{eq,LI}[i] \tag{22}$$

$$P_{eq,S}[i] = V_S[i] \cdot I_{eq,S}[i] = V_S[i] \cdot I_S[i] \tag{23}$$

In the problem formulation, we use $P_{eq,LA}[i]$, $P_{eq,LI}[i]$, and $P_{eq,S}[i]$ $(1 \le i \le N)$ as the optimization variables instead of the EES array current profiles $I_{LA}[i]$, $I_{LI}[i]$, $I_S[i]$ $(1 \le i \le N)$. This will transform the problem into a convex CSP as we shall see in the following. The HEES controller can easily calculate the values of control variables $I_{LA}[i]$, $I_{LI}[i]$, $I_S[i]$ $(1 \le i \le N)$ from the derived values of $P_{eq,LA}[i]$, $P_{eq,LI}[i]$, and $P_{eq,S}[i]$ using Eqns. (11), (21) – (23).

We rewrite constraint (14) as follows to make it a convex inequality constraint:

$$P_{bus,LA}[i] + P_{bus,LI}[i] + P_{bus,S}[i] \le P_{src}[i] \cdot \eta_{conv,src} - \frac{P_{load}[i]}{\eta_{conv,load}} \tag{24}$$

Both the energy conservation law and the load power requirement are still satisfied in (24). We know that $P_{bus,LA}[i]$, $P_{bus,LI}[i]$, and $P_{bus,S}[i]$ are convex functions of $P_{eq,LA}[i]$, $P_{eq,LI}[i]$, and $P_{eq,S}[i]$, respectively, from Eqns. (11) and (13). This proves that constraint (24) is a convex inequality constraint. Moreover, the other constraints (16) – (20) can be translated into linear inequality constraints of $P_{eq,LA}[i]$, $P_{eq,LI}[i]$, and $P_{eq,S}[i]$ $(1 \le i \le N)$. Details are omitted due to space limitation.

Then the feasibility check problem becomes a convex CSP [19] because all the constraints are convex (or linear) inequality constraints. We set the objective function to be a constant value $Const$ in order to solve this feasibility check problem using standard convex optimization tools such as CVX [19]. After the feasibility check, we calculate the average SoC levels $SoC_{avg,LA}$ and $SoC_{avg,LI}$ of the lead-acid battery array and the Li-ion battery array, respectively, from the derived $P_{eq,LA}[i]$ and $P_{eq,LI}[i]$ profiles. These average SoC values are important in the subsequent optimization step.

2) Minimizing the Overall Value Degradation

We perform optimization to find the optimal values of $P_{eq,LA}[i]$, $P_{eq,LI}[i]$, and $P_{eq,S}[i]$ $(1 \le i \le N)$ in order to minimize the overall value degradation given by Eqn. (15). We make use of the following observation in deriving the near-optimal charge management policy:

Observation III: Notice that it is possible to decouple the charging and discharging profile of a (lead-acid or Li-ion) battery array into a set of charging/discharging cycles. The cycle with the largest SoC swing has the most significant contribution to the SoH degradation.

Based on Observation III, we focus on minimizing the overall value degradation induced by the charging/discharging cycle (after decoupling) with the largest SoC swing for both battery arrays. Minimizing this objective function helps in minimizing the overall value degradation induced by the other charging/discharging cycles as well. Of course, when calculating the SoH degradation during an operation period, the novel model derived in Section III.B is used.

For the lead-acid battery array, the largest SoC swing in all the charging/discharging cycles is given by:

$$SoC^{MAX}_{swing,LA} = \max_{1 \le j \le i \le N} \left| \frac{\sum_{k=j}^{i} I_{eq,LA}[k] \cdot \Delta_T}{C_{full,LA}} \right| \tag{25}$$

$SoC^{MAX}_{swing,LA}$ is a convex function of $P_{eq,LA}[i]$ $(1 \le i \le N)$ because the pointwise maximum function of a set of convex function is still a convex function [19]. Similarly, we define and calculate the largest SoC swing $SoC^{MAX}_{swing,LI}$ for the Li-ion battery array. Moreover, let $D_{SoH,cycle,LA}(SoC_{swing}, SoC_{avg})$ denote the SoH degradation of the lead-acid battery array in one charging/discharging cycle as a function of the SoC swing SoC_{swing} and average SoC level SoC_{avg}. Similarly, we define the function $D_{SoH,cycle,LI}(SoC_{swing}, SoC_{avg})$ for the Li-ion battery array. We minimize the overall value degradation contributed by the charging/discharging cycles with largest SoC swing for both battery arrays, as an estimation of the original objective function (15). The objective is given by:

$$Cost_{LA} \cdot \frac{D_{SoH,cycle,LA}(SoC^{MAX}_{swing,LA}, SoC_{avg,LA})}{D_{SoH,end}} + Cost_{LI} \cdot \frac{D_{SoH,cycle,LI}(SoC^{MAX}_{swing,LI}, SoC_{avg,LI})}{D_{SoH,end}} \tag{26}$$

where we use average SoC levels obtained from the feasibility check as estimation of average SoC levels $SoC_{avg,LA}$ and $SoC_{avg,LI}$ in (26). Objective function (26) is a convex function of $P_{eq,LA}[i]$ and $P_{eq,LI}[i]$ $(1 \le i \le N)$ because: (i) $D_{SoH,cycle,LA}(SoC_{swing}, SoC_{avg})$ and $D_{SoH,cycle,LI}(SoC_{swing}, SoC_{avg})$ are convex and monotonically increasing functions of SoC_{swing} when SoC_{avg} is given, and (ii) $SoC^{MAX}_{swing,LA}$ and $SoC^{MAX}_{swing,LI}$ are convex functions of $P_{eq,LA}[i]$ and $P_{eq,LI}[i]$ $(1 \le i \le N)$, respectively, as mentioned before.

The constraints of this optimization problem are the same as those in the feasibility check problem. Therefore, the overall value degradation minimization described in this part is a convex optimization problem because it has convex objective function and convex inequality constraints. We find the optimal solution of this problem in polynomial time complexity.

After we minimize the overall value degradation induced by the charging/discharging cycle (after decoupling) with the largest SoC swing of both battery arrays, we will continue to minimize the effect on the overall value degradation from the other charging/discharging cycles. However, detailed discussion is out of scope of this paper.

VI. Experimental Results

We derive and implement the proposed SoH-aware charge management policy on a typical HEES system comprised of a lead-acid battery bank, a Li-ion battery bank, and a supercapacitor bank. The lead-acid battery bank has 3 Ah nominal capacity and 20 V terminal voltage. The Li-ion battery bank has 4 Ah nominal capacity and 15 V terminal voltage. The supercapacitor bank has 200 F capacitance. The energy capacity of the supercapacitor array is 10% of that of the battery array. The SoH-aware control policy minimizes the overall value degradation in the propose HEES system.

We compare the cycle life of the proposed system with two baseline systems. Baseline 1 uses a HEES system comprised of a lead-acid battery bank and a Li-ion battery bank that are the same as the proposed system, but without the supercapacitor bank. Baseline 2 uses the same HEES system as the proposed system. Both baseline systems exploit the optimal HEES control policy in order to satisfy the load power requirement and improve the HEES system cycle efficiency. The load power requirement is satisfied in all systems.

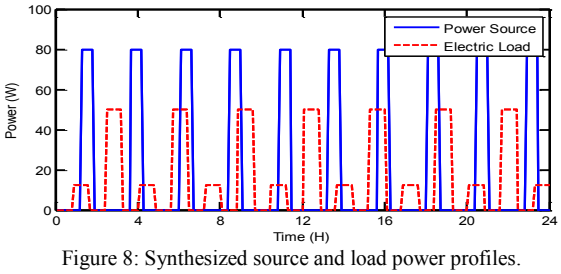

Figure 8: Synthesized source and load power profiles.

We perform experiments based on two sets of source and load power profiles. In the first experiment, we use synthesized source and load power profiles as shown in Figure 8. We compare the SoH degradation and cycle life of both battery arrays between the proposed

system and two baseline systems, with results shown in Table I. The proposed system achieves significantly smaller SoH degradation rate, and hence, larger cycle life, compared with both baseline systems. It achieves a cycle life improvement up to 17.3X compared with Baseline 1 thanks to the contributions of both the supercapacitor bank and the SoH-aware control policy. On the other hand, the maximum cycle life improvement compared with Baseline 2 is 3.5X due to the SoH-aware control policy solely.

Table I. SoH degradation and cycle life comparison between the proposed system and baseline systems using synthesized power profiles.

		Compare with Baseline 1	Compare with Baseline 2
Lead-acid	SoH degradation	10.6%	33.2%
	Cycle life	9.4X	3.0X
Li-ion	SoH degradation	5.8%	28.7%
	Cycle life	17.3X	3.5X

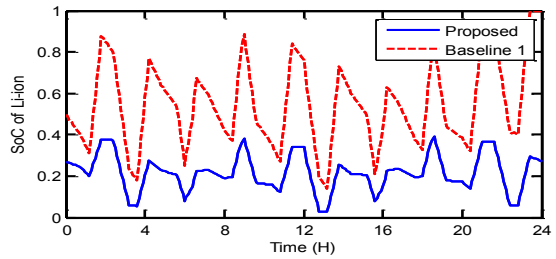

Figure 9: SoC profiles of the Li-ion battery array of the proposed system and Baseline 1 under synthesized power profiles.

We provide the SoC profile versus time for the proposed system and Baseline 1 as shown in Figure 9. The maximum SoC swing and average SoC level of the Li-ion battery array have been reduced by 35% and 30%, respectively. The former accounts for about 6X improvement in cycle life whereas the latter accounts for about 3X improvement.

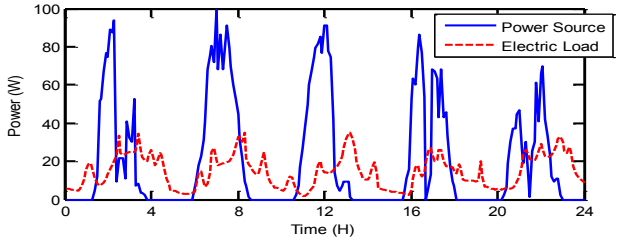

Figure 10: Real source and load power profiles.

Table II. SoH degradation and cycle life comparison between the proposed system and baseline systems using real power profiles.

		Compare with Baseline 1	Compare with Baseline 2
Lead-acid	SoH degradation	7.4%	24.2%
	Cycle life	13.5X	4.1X
Li-ion	SoH degradation	7.2%	22.8%
	Cycle life	13.9X	4.4X

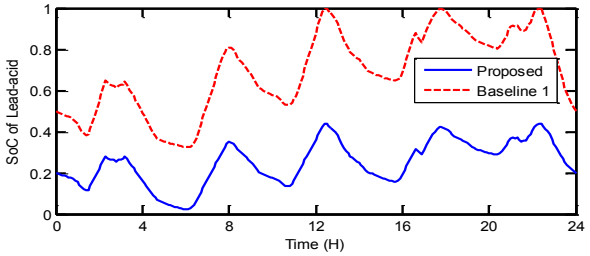

Figure 11: SoC profiles of the lead-acid battery array in the proposed system and Baseline 1 under real power profiles.

In the second experiment, we use actual source and load power profiles scaled for the proposed HEES system, as shown in Figure 10. We compare the SoH degradation and cycle life of both battery arrays between the proposed system and two baseline systems, with results shown in Table II. The proposed system achieves a cycle life improvement up to 13.9X. Similarly, we provide the SoC profile of the lead-acid battery array versus time in the proposed system and Baseline 1 as shown in Figure 11.

VII. Conclusion

Cycle life of EES elements is one of the most important metrics that should be considered. Cycle life is related to SoH degradation. SoH degradation models presented in the reference papers can only be applied in the cases of constant-current cycled charging and discharging with the same SoC swing in each cycle. This work is the first attempt to derive a novel SoH degradation model that estimates SoH degradation rate under arbitrary charging and discharging patterns of a battery. We also introduce a near-optimal charge management policy based on the proposed SoH degradation model focusing on extending cycle life of the batteries in the HEES systems while simultaneously improving the overall cycle efficiency. The derivation procedure of the SoH-aware charge management policy is based on the convex optimization technique.

References

[1] J. Baker and A. Collinson, "Electrical energy storage at the turn of the millennium," *Power Engineering Journal*, 1999.

[2] T. Moore and J. Douglas, "Energy storage, big opportunities on a smaller scale," *EPRI J.*, 2006.

[3] M. Pedram, N. Chang, Y. Kim, and Y. Wang, "Hybrid electrical energy storage systems," in *ISLPED*, 2010.

[4] F. Koushanfar, "Hierarchical hybrid power supply networks," in *Design Automation Conference* (DAC), 2010.

[5] Y. Wang, Y. Kim, Q. Xie, N. Chang, and M. Pedram, "Charge migration efficiency optimization in hybrid electrical energy storage (HEES) systems," in *ISLPED*, 2011.

[6] Q. Xie, Y. Wang, Y. Kim, N. Chang, and M. Pedram, "Charge allocation for hybrid electrical energy storage systems," in *CODES+ISSS*, 2011.

[7] Q. Xie, Y. Wang, M. Pedram, Y. Kim, D. Shin, and N. Chang, "Charge replacement in hybrid electrical energy storage systems," in *Asia and Pacific Design Automation Conference* (ASP-DAC), 2012.

[8] A. Millner, "Modeling Lithium Ion battery degradation in electric vehicles," *IEEE CITRES*, 2010.

[9] M. Dubbary, V. Svoboda, R. Hwu, and B. Liaw, "Capacity and power fading mechanism identification from a commercial cell evaluation," *Journal of Power Sources*, 2007.

[10] G. Sikha, R. Ramadass, B. Haran, R. White, and B. Popov, "Comparison of the capacity fade of Sony US18650 cells charged with different protocols," *Journal of Power Sources*, 2003.

[11] J. Li, E. Murphy, J. Winnick, and P. Kohl, "The effects of pulse charging on cycle characteristics of commercial lithium-ion batteries," *Journal of Power Sources*, 2001.

[12] Y. Liu, C. Hsieh, and Y. Luo, "Search for an optimal five-step charging pattern for Li-ion batteries using consecutive orthogonal arrays," *IEEE Trans. on Energy Conversion*, 2011.

[13] Q. Xie, X. Lin, Y. Wang, M. Pedram, D. Shin, and N. Chang, "State of health aware charge management in hybrid electrical energy storage systems," in *Design, Automation, and Test in Europe* (DATE), 2012.

[14] S. Peterson, J. Apt, and J. Whitacre, "Lithium-ion battery cell degradation resulting from realistic vehicle and vehicle-to-grid utilization," *Journal of Power Sources*, 2010.

[15] Q. Zhang and R. White, "Capacity fade analysis of a lithium ion cell," *Journal of Power Sources*, 2008.

[16] P. Rong and M. Pedram, "An analytical model for predicting the remaining battery capacity of Lithium-ion batteries," *IEEE Trans. on VLSI Systems*, 2006.

[17] D. Zhu, Y. Wang, S. Yue, Q. Xie, N. Chang, and M. Pedram, "Maximizing return on investment of a grid-connected hybrid electrical energy storage system," *ASP-DAC*, 2013.

[18] D. Linden and T. B. Reddy, *Handbook of Batteries*, McGraw-Hill Professional, 2001.

[19] S. Boyd and L. Vandenberghe, *Convex Optimization*, Cambridge University Press, 2004.